



Since January 2020 Elsevier has created a COVID-19 resource centre with free information in English and Mandarin on the novel coronavirus COVID-19. The COVID-19 resource centre is hosted on Elsevier Connect, the company's public news and information website.

Elsevier hereby grants permission to make all its COVID-19-related research that is available on the COVID-19 resource centre - including this research content - immediately available in PubMed Central and other publicly funded repositories, such as the WHO COVID database with rights for unrestricted research re-use and analyses in any form or by any means with acknowledgement of the original source. These permissions are granted for free by Elsevier for as long as the COVID-19 resource centre remains active.



ELSEVIER

Contents lists available at ScienceDirect

Virology

journal homepage: www.elsevier.com/locate/yviro

Extracellular signal-regulated kinase (ERK) activation is required for porcine epidemic diarrhea virus replication

Youngnam Kim, Changhee Lee*

Animal Virology Laboratory, School of Life Sciences, BK21 plus KNU Creative BioResearch Group, Kyungpook National University, Daegu 702-701, Republic of Korea



ARTICLE INFO

Article history:

Received 23 April 2015

Returned to author for revisions

28 May 2015

Accepted 4 June 2015

Available online 23 June 2015

Keywords:

PEDV

ERK1/2

Elk-1

Signal transduction

Viral replication

ABSTRACT

Porcine epidemic diarrhea virus (PEDV) is a highly enteropathogenic coronavirus of swine that causes acute enteritis with high mortality in nursery piglets. To date, the cellular factors involved in PEDV replication have not been well defined. The extracellular signal-regulated kinase (ERK) that serves as a critical component of cellular signal transduction pathways to modulate a variety of cellular functions has been shown to regulate several viral infections. In the present study, we found that PEDV activates ERK1/2 early in infection independently of viral replication. The PEDV-induced ERK1/2 activation resulted in the phosphorylation of its downstream substrate Elk-1 in infected cells. Treatment with ERK inhibitors or ERK1/2 knockdown significantly suppressed viral progeny production. Inhibition of ERK activation also diminished viral protein expression and genomic and subgenomic RNA transcription. These findings indicate that the ERK signaling pathway plays an important role in the PEDV life cycle and beneficially contributes to viral infection.

© 2015 Elsevier Inc. All rights reserved.

Introduction

Porcine epidemic diarrhea (PED) is an emerging and important swine disease that causes acute enteritis with high mortality in piglets (Debouck and Pensaert, 1980; Pijpers et al., 1993; Saif et al., 2012). PED is characterized by severe villous atrophy in the small intestine, which is more serious in newborn pigs than in older pigs, resulting in malabsorptive watery diarrhea followed by fatal dehydration in piglets (Madson et al., 2014; Saif et al., 2012; Shibata et al., 2000). The associated mortality rates vary depending on age likely due to age-dependent disease severity and generally approach 90–100% in 1- to 3-day-old neonatal piglets (Saif et al., 2012). The disease was first observed in the United Kingdom in 1971 and then spread to multiple swine-producing European countries (Chasey and Cartwright, 1978; Oldham, 1972; Pensaert et al., 1981). In Asia, PED epidemics first occurred in 1982 and since then, PED remains a major concern in Asian countries, particularly in China and South Korea (Chen et al., 2008; Kweon et al., 1993; Li et al., 2012; Puranaveja et al., 2009; Sun et al., 2012; Takahashi et al., 1983). During 2013 and 2014, a severe large-scale PED epizootic emerged in the United States and re-emerged in

South Korea, Taiwan, and Japan, which led to tremendous financial losses in the pork industries in these countries (Lee and Lee, 2014; Lee et al., 2014a, 2014b; Lin et al., 2014; Mole, 2013; Stevenson et al., 2013).

The etiological agent of PED, the PED virus (PEDV), was identified in 1978 as a coronavirus, which is a member of the genus *Alphacoronavirus* within the family *Coronaviridae* of the order *Nidovirales* (Pensaert and de Bouck, 1978; Saif et al., 2012). PEDV is a large, enveloped virus possessing a single-stranded positive-sense RNA genome, approximately 28 kb long, with a 5' cap and a 3' polyadenylated tail (Pensaert and de Bouck, 1978; Saif et al., 2012). The PEDV genome is composed of a 5' untranslated region (UTR), at least 7 open reading frames (ORF1a, ORF1b, and ORF2 through 6), and a 3' UTR (Kocherhans et al., 2001). The two large ORF1a and 1b comprising the 5' two-thirds of the genome encode non-structural proteins (nsps). The remaining ORFs in the 3' terminal region code for four major structural proteins, the 150–220 kDa glycosylated spike (S) protein, 20–30 kDa membrane (M) protein, 7 kDa envelop (E) protein, and 58 kDa nucleocapsid (N) protein (Duarte et al., 1994; Saif et al., 2012). PEDV infection is initiated by binding of the viral S protein to the receptor on host cells, and the viral genome is released into the cytoplasm after the viral entry process. As positive-strand RNA viruses, the PEDV genome functions as an mRNA for the synthesis of viral proteins. Translation initially occurs from ORF1a and ORF1b, yielding the 1a and 1b replicase polyproteins, with the latter produced by a –1 ribosomal frame shift. These polyproteins are

* Corresponding author at: School of Life Sciences, College of Natural Sciences, Kyungpook National University, Daegu 702-701, Republic of Korea. Tel.: +82 53 950 7365; fax: +82 53 955 5522.

E-mail address: changhee@knu.ac.kr (C. Lee).

subsequently cleaved into functional 16 nsps including the viral RNA-dependent RNA polymerase (RdRp). The RdRp-containing replication complex in turn mediates viral genomic RNA synthesis and subgenomic (sg) mRNA transcription, eventually producing a nested set of 3' co-terminal sg mRNAs that are individually translated to structural proteins (Lai et al., 2007; Saif et al., 2012). A recent report has shown that PEDV induces caspase-independent apoptosis through the activation of mitochondrial apoptosis-inducing factor (AIF) to facilitate viral replication and pathogenesis (Kim and Lee, 2014). However, whether other cellular factors or mechanisms may also regulate PEDV infection is still unknown.

The mitogen-activated protein kinase (MAPK) cascade pathways are central building blocks in the intracellular signaling network. As the global cellular regulators in response to various extracellular stimuli, the MAPK pathways transmit signals to diverse intracellular targets and exquisitely control numerous cellular activities. The extracellular signaling-regulated kinase (ERK) signaling pathway is one of the three MAPK cascades that play important roles in the regulation of various cellular processes (Garrington and Johnson, 1999; Roux and Blenis, 2004). Activation of the ERK pathway includes three signal cascades, Raf, MEK1/2, and ERK1/2. Upon stimulation, the Raf/MEK/ERK cascade is initiated by receptor tyrosine kinases that signal through the small GTP-binding protein Ras. This event results in Raf activation that binds to and phosphorylates the dual specificity kinases MEK1/2, which in turn activates ERK1/2 by phosphorylation. The activated ERK1/2 finally translocates into the nucleus and phosphorylates numerous downstream substrates including transcription factors regulating transcription for a large number of genes. Therefore, the ERK pathway modulates a wide range of important cellular functions, such as cell proliferation, differentiation, survival and apoptosis (Roux and Blenis, 2004; Shaul and Seger, 2007). Since viruses are obligate intracellular parasites, they may regulate such functions to benefit their own multiplication in host cells by manipulating the ERK signaling pathway. In fact, several viruses have been shown to exploit the host ERK signaling pathway for optimal viral replication and gene expression (Cai et al., 2007; Lee and Lee, 2010; Lim et al., 2005; Marjuki et al., 2006; Moser and Schultz-Cherry, 2008; Schümann and Döbelstein, 2006; Wang et al., 2006; Wei and Liu, 2009; Zampieri et al., 2007). However, the role of the ERK signaling pathway in PEDV replication has not been determined.

In the present study, we tried to examine whether PEDV infection activates the ERK signaling pathway in cultured cells and ERK activation is involved in PEDV replication. It was found that PEDV induces early strong and transient activation of ERK1/2 that is independent of maximal viral gene expression. Furthermore, UV-inactivated virus was sufficient to trigger ERK1/2 activation, indicating the absence of a critical action of viral replication for its phosphorylation. PEDV production was significantly impaired by MEK inhibitors and ERK1/2-specific siRNA. Further experiments revealed that independent treatment with each MEK inhibitor resulted in the distinct reduction of viral RNA synthesis and viral protein translation but did not affect viral entry. In addition, inhibition of ERK activation had no effect on PEDV-induced apoptotic cell death. Together, our data demonstrate a pivotal role for the ERK signaling pathway in a post-attachment stage of the PEDV life cycle.

Results

PEDV activates ERK1/2

In order to investigate the effect of PEDV on the ERK1/2 signaling cascade, the kinetics of ERK1/2 phosphorylation was monitored in Vero cells infected with PEDV at an MOI of 1 at different times postinfection by Western blot analysis. As shown in

Fig. 1 A, only small amounts of activated ERK1/2 were detected in mock-infected Vero cells as a negative control. This was considered the background level of phosphorylated ERK1/2 (pERK1/2), possibly in response to the components of the media. In contrast, PEDV infection significantly stimulated ERK1/2 activity by 6 h postinfection (hpi) that was most markedly induced at 12 hpi and then dramatically decreased at 24 hpi, returning to the baseline level thereafter. In addition, the activation profile of ERK1/2 was comparably observed in cells infected with PEDV at an MOI of 0.1 (data not shown). These results indicated that PEDV infection triggers early strong but transient activation of ERK1/2. Interestingly, new viral protein synthesis was first evident by 12 hpi (Fig. 1A), while the maximal phosphorylation status of ERK1/2 was also seen at this time point, suggesting that ERK1/2 activation occurs independently of PEDV replication. These data further allowed us to assume that ERK1/2 regulation of the PEDV replication cycle occurs at early events in virus infection, prior to the considerable protein production obvious at late time points. To demonstrate this hypothesis, Vero cells were treated with an equal amount of UV-irradiated inactivated virus that is capable of allowing viral attachment and internalization, but incapable of pursuing viral gene expression (Fig. 1B). UV-inactivated PEDV efficiently induced ERK1/2 activation which was comparable to the phosphorylation pattern observed in PEDV-infected cells (Fig. 1B). Therefore, inactivated PEDV infection was found to be still sufficient to activate the ERK signaling pathway, suggesting that initial entry events in the virus life cycle may be responsible for early ERK activation.

Next, we tried to further confirm the levels of ERK1/2 phosphorylation in cells infected with PEDV or treated with UV-inactivated PEDV by using a Fast Activated Cell-Based ELISA (FACE) assay. Consistent with the results described above, there was most significantly increased in the ERK1/2 phosphorylation at 12 h after PEDV infection, showing an approximately 5-fold higher level of phosphorylation than that in the mock-infected cells (Fig. 1C). Moreover, the activation pattern of pERK1/2 was virtually the same in the UV-irradiated PEDV-exposed cells as in the non-irradiated PEDV-infected cells (Fig. 1D). In addition, the levels of total ERK1/2 remained unchanged in the cells infected with PEDV and inactivated PEDV at various time points after infection when compared to levels in mock-infected cells. Altogether, our results demonstrated that PEDV replication was not required for ERK1/2 phosphorylation.

PEDV triggers nuclear translocation of activated ERK1/2 and leads to Elk-1 phosphorylation

Upon stimulation, a significant population of ERK molecules accumulates in the nucleus and activates a series of transcription factors. To investigate how ERK1/2 activation following PEDV infection proceeds in such a cascade, we first examined the subcellular localization of pERK1/2 in cells infected with PEDV and UV-inactivated PEDV (Fig. 2). In mock-infected cells, no active ERK1/2 was detected in any cellular compartments during the entire period of the experiment (Fig. 2A and B, top panels). In contrast, at 6 hpi, pERK1/2 showed distinct nuclear staining with a weak punctuate cytoplasmic signal and was continuously detected in the nucleus by 24 hpi (Fig. 2A). As PEDV replication progressed, however, punctuate cytoplasmic staining of active ERK1/2 was dispersed and maintained by 24 hpi. Similarly, after exposure of cells to UV-inactivated PEDV, the majority of pERK1/2 exhibited a nuclear distribution with diffusely punctuate cytoplasmic staining. This localization pattern of active ERK molecules remained unchanged by 24 h after inactivated PEDV infection (Fig. 2B). Given that Elk-1 is one of the transcription factors phosphorylated by the ERK signaling pathway (Shaul and Seger, 2007; Wei and Liu, 2009), we measured the activation status of Elk-1 following PEDV-induced ERK activation (Fig. 3). No

activation of Elk-1 was detected in mock-infected cells. In contrast, PEDV infection resulted in the phosphorylation of Elk-1 with kinetics that identically paralleled those observed in ERK1/2 activation (Fig. 3A). Furthermore, cells exposed to UV-inactivated PEDV showed a phosphorylated Elk-1 profile comparable to that in PEDV-infected cells (Fig. 3B). This result indicated that these ERK signaling molecules that were activated following PEDV infection cooperates in reaching their appropriate downstream destinations to function as key regulators of inducible cellular processes.

ERK1/2 activation regulates PEDV replication

To examine the biological importance of ERK1/2 activation in PEDV infection, specific inhibitors of the ERK signaling pathway were used. Vero cells were pretreated with the MEK1/2 inhibitor U0126 or PD98059 at various concentrations or with DMSO (0.5%) as a vehicle control for 1 h prior to infection. The inhibitor or DMSO was present during the entire period of infection. The

cytotoxicity of the MEK inhibitors was determined by the MTT assay in Vero cells. All doses of the inhibitors tested in the present study caused no detectable cell death in Vero cells (data not shown). Viral production was initially measured by monitoring the cytopathic effect (CPE) after infection and was confirmed by immunofluorescence using N protein-specific MAb at 48 hpi (Fig. 4). In vehicle-treated control cells, visible CPE appeared at 24 hpi and became predominant by 48 hpi, and N-specific staining was clearly evident in many cell clusters, indicating infection and the spread of the virus to neighboring cells. In contrast, the inhibitory effect of U0126 and PD98059 on virus propagation was readily detectable. As shown in Fig. 4A, each inhibitor significantly decreased PEDV-induced CPE (first panels) and viral gene expression (second panels) in a dose-dependent manner. As quantified by N protein staining results, the percentage of virus-infected cells was similarly reduced during independent treatment with each inhibitor, resulting in a maximal 80% inhibition at the highest concentration used (Fig. 4B). PD98059 prevents ERK1/2

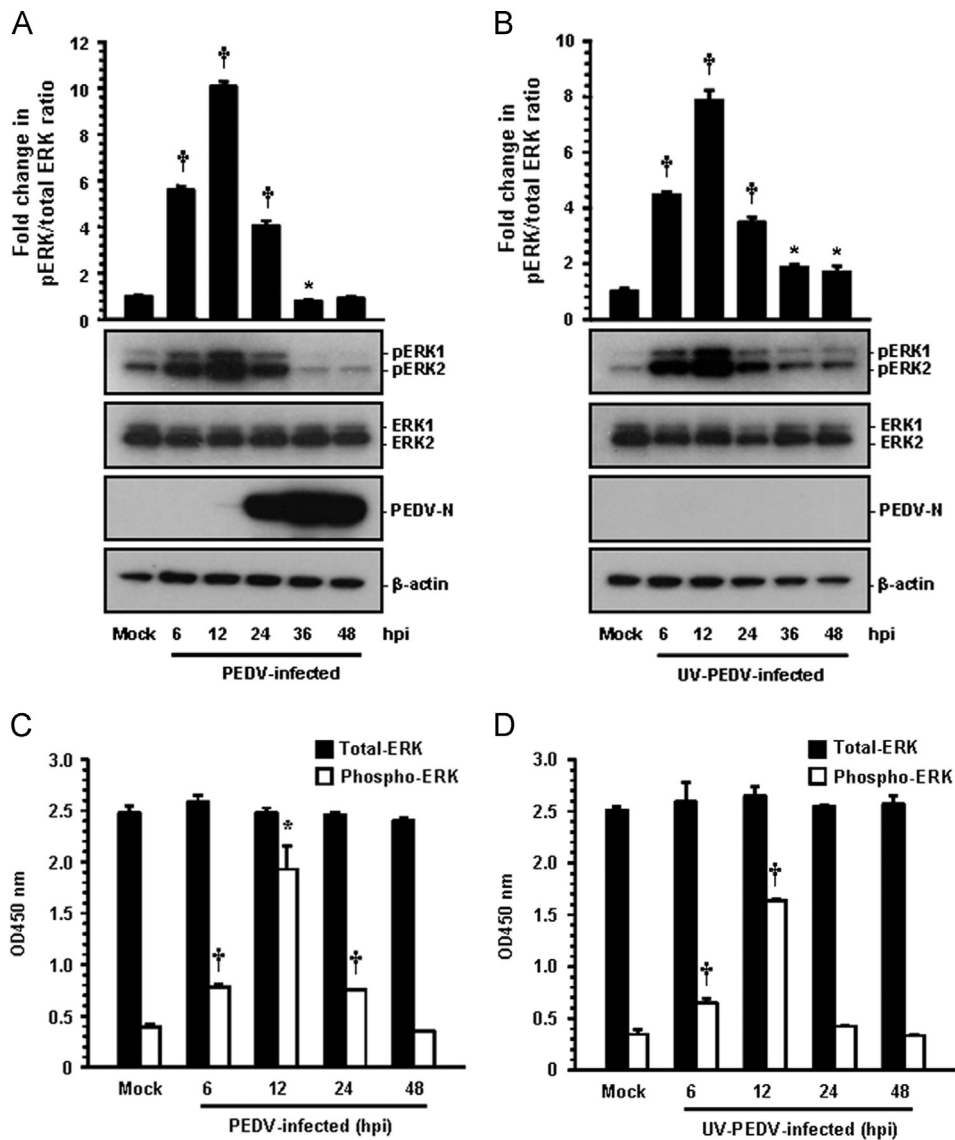


Fig. 1. PEDV activates the ERK1/2 signaling pathway in cultured cells. Vero cells were mock infected or infected with PEDV at an MOI of 1 or an equal amount of UV-inactivated PEDV. (A and B) Whole cell lysates were prepared for the indicated times following PEDV infection (hpi) and subjected to Western blot analysis with the antibody specific for phosphorylated ERK1/2 (pERK1/2), ERK1/2, or the PEDV N protein. The blot was also reacted with mouse MAb against β -actin to verify equal protein loading. Fold changes in the pERK1/2:total ERK1/2 ratio are plotted. (C and D) ERK1/2 activation induced by PEDV infection was quantitatively determined using a FACE assay. Vero cells were fixed at the indicated time points with 4% formaldehyde and incubated with an anti-ERK1/2 or anti-pERK1/2 antibody followed by HRP-conjugated IgG antibodies. The absorbance of the solution was determined at 450 nm using a spectrophotometer. These results are representative of the results of three independent experiments and error bars represent standard deviations. *, $P=0.001$ to 0.05; †, $P < 0.001$.

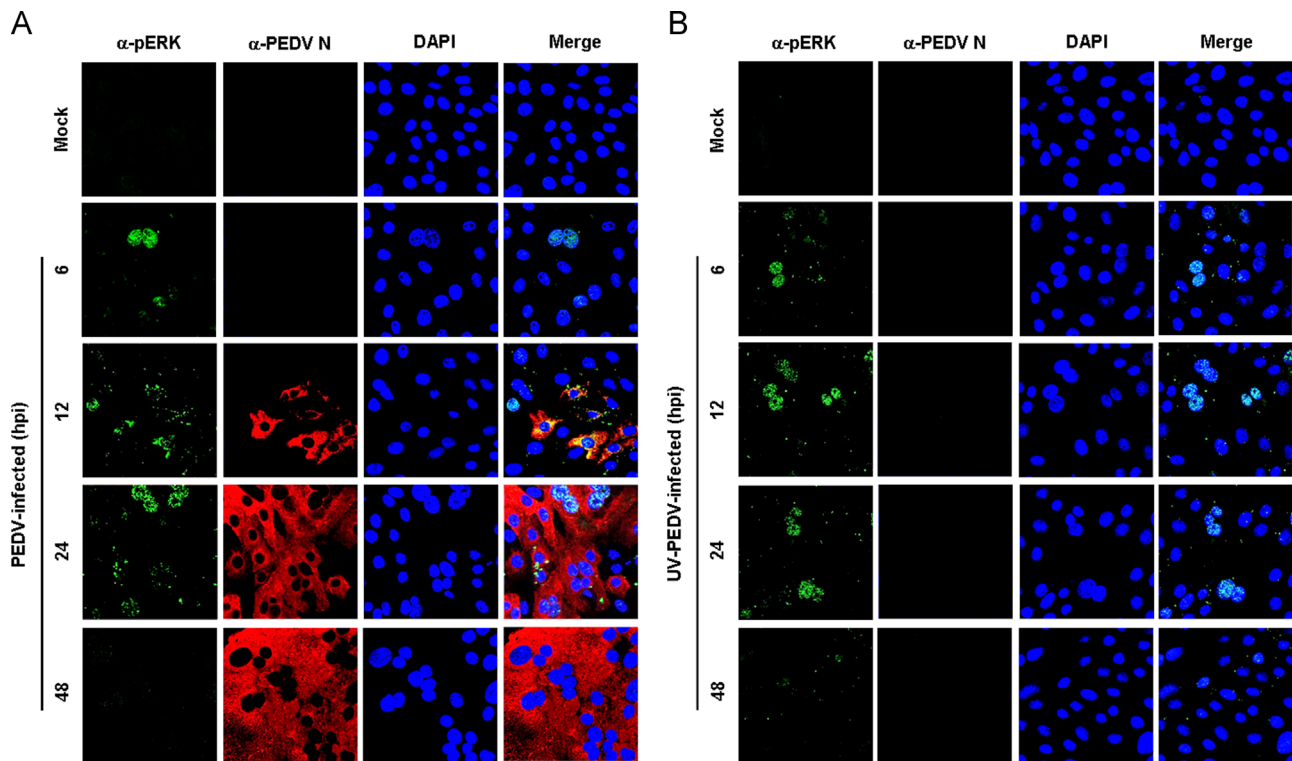


Fig. 2. PEDV induces nuclear translocation of pERK1/2. Vero cells were mock infected or infected with PEDV (A) or UV-inactivated PEDV (B). At the indicated time points, infected cells were fixed and labeled with antibodies against pERK1/2 (green) and PEDV N (red). The cells were then counterstained with DAPI, and the intracellular localization of pERK1/2 in virus-infected cells was examined using a confocal microscope at 400 \times magnification.

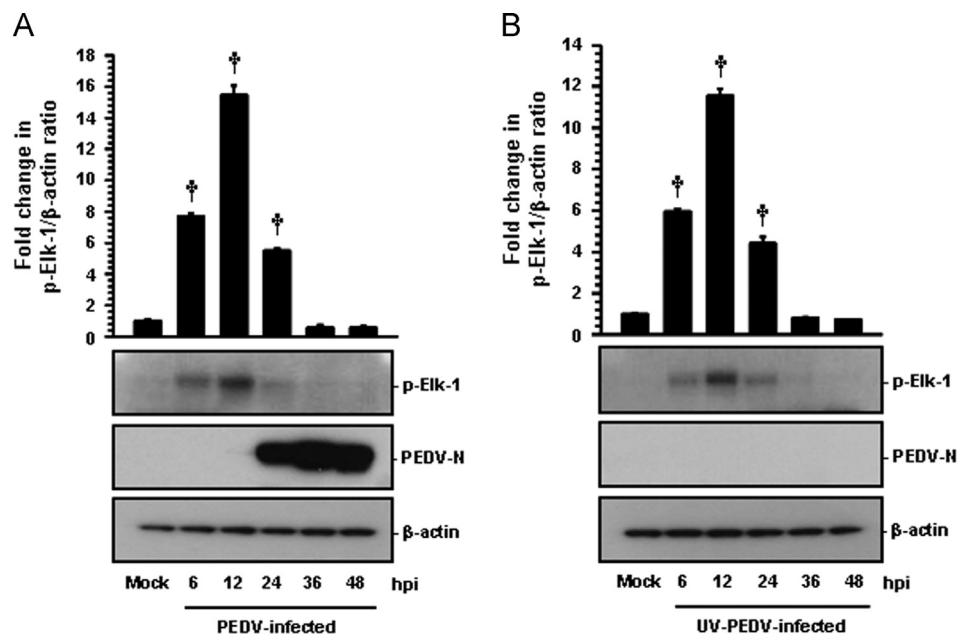


Fig. 3. Phosphorylated ERK1/2 leads to the activation of downstream target Elk-1. Vero cells were mock infected or infected with PEDV at an MOI of 1 (A) or an equal amount of UV-inactivated PEDV (B). Whole cell lysates were prepared for the indicated times following PEDV infection (hpi) and subjected to Western blot analysis with the antibody to pElk-1 or PEDV N. The blot was also reacted with mouse MAb against β -actin to verify equal protein loading. Fold changes in the pElk-1: β -actin ratio are plotted. These data are representative of the results of three independent experiments and error bars represent standard deviations. †, $P < 0.001$.

activation by blocking phosphorylation of MEK1/2, whereas U0126 is not only capable of blocking the activation of MEK1/2 but also inhibiting MEK1/2 activity (Alessi et al., 1995; Davis et al., 2000). Therefore, U0126 is a more potent inhibitor of ERK1/2 activation than PD98059 (Favata et al., 1998). Our data also revealed that

U0126 was significantly more effective in inhibiting PEDV production (an 80% reduction in virus propagation at a concentration of 20 μ M) than PD98059 (a 20% reduction in virus propagation at the same concentration). To further show relevance, we determined the activation status of ERK1/2, the downstream activator of

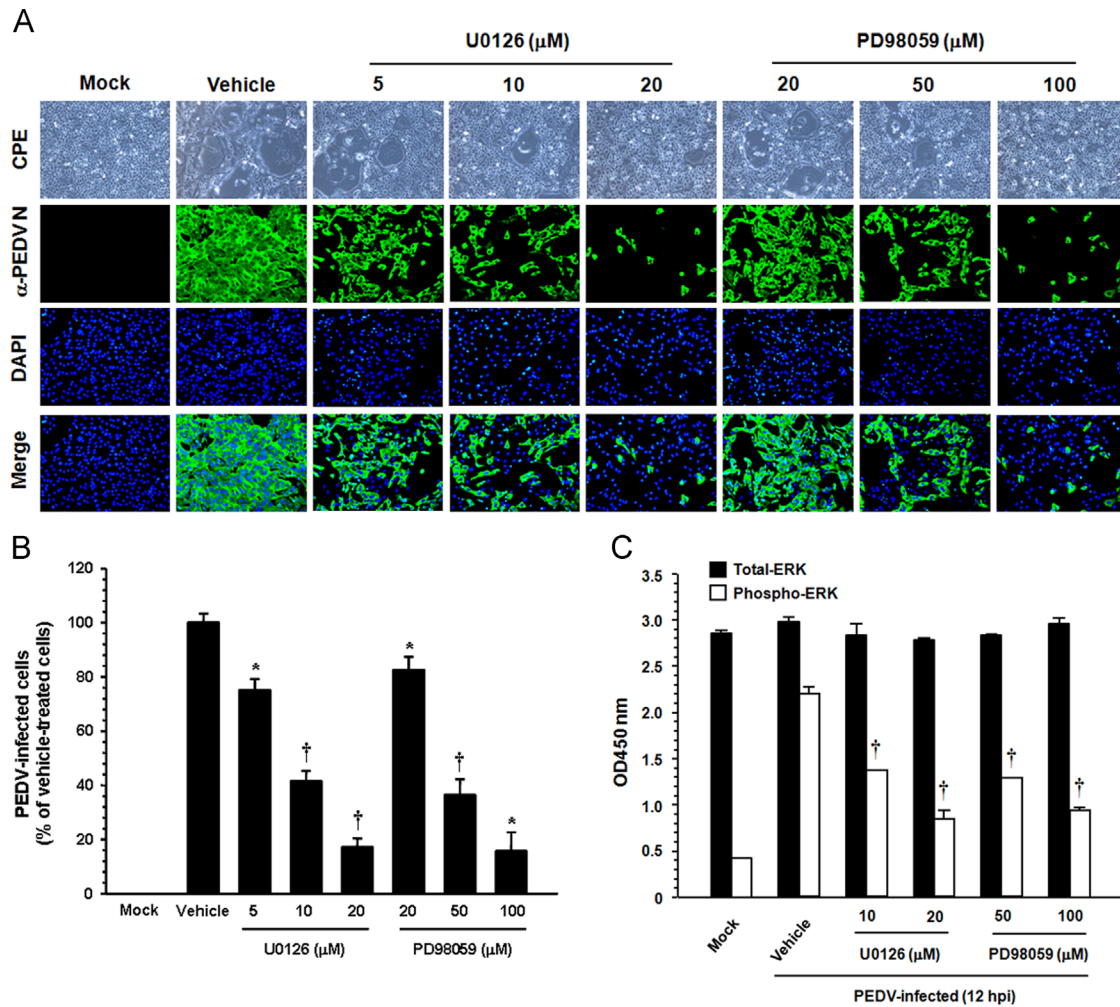


Fig. 4. PEDV propagation is suppressed by inhibition of ERK1/2 activation. (A) Vero cells were preincubated with DMSO, U0126 (5, 10, and 20 μM), or PD98059 (20, 50, and 100 μM) for 1 h prior to infection and were mock-infected or infected with PEDV at an MOI of 1. Virus-infected cells were further maintained for 48 h in the presence of DMSO or inhibitors. PEDV-specific CPEs were observed daily and were photographed at 48 hpi using an inverted microscope at a magnification of $100\times$ (first panels). For immunostaining, infected cells were fixed at 48 hpi and incubated with MAb against the N protein, followed by Alexa green-conjugated goat anti-mouse secondary antibody (second panels). The cells were then counterstained with DAPI (third panels) and examined using a fluorescent microscope at $200\times$ magnification. (B) Viral production in the presence of each inhibitor was measured by quantifying the percentage of cells expressing N proteins through flow cytometry. Values shown are representative of three independent experiments and error bars represent standard deviations. (C) Chemical inhibition of ERK1/2 activation was quantitatively determined using FACE assay. Vero cells were mock-infected or PEDV-infected in the presence of DMSO, U0126 (10 and 20 μM), or PD98059 (50 and 100 μM). The cells were fixed at 12 hpi with 4% formaldehyde and incubated with an anti-ERK1/2 or anti-pERK1/2 antibody followed by HRP-conjugated IgG antibodies. The absorbance of the solution was determined at 450 nm using a spectrophotometer. These results represent the results of three independent experiments and error bars represent standard deviations. *, $P=0.001$ to 0.05; †, $P < 0.001$.

MEK1/2, after treatment with two MEK inhibitors in PEDV-infected cells. Both inhibitors were found to markedly decrease levels of pERK1/2 at 12 hpi (Fig. 4C). However, the inhibitory effect of the two inhibitors was inconsistent, with a significant inhibition observed for U0126 and PD98059 at 10 μM and 50 μM , respectively. This finding indicated that the effect of both inhibitors on virus production correlates with the ability of each compound to inhibit ERK1/2 phosphorylation. Taken together, these data demonstrated that treating cells with each MEK inhibitor hampered the activation of ERK1/2 and accordingly suppressed PEDV propagation, suggesting that the Raf/MEK/ERK signaling pathway plays a role in PEDV replication.

In addition, virus yield was determined during treatment with the two MEK inhibitors to assess whether ERK activity is truly necessary for PEDV replication. Upon infection, viral supernatants were collected at 48 hpi and viral titers were measured. As Fig. 5A shows, the presence of each inhibitor reduced the release of viral progeny in a dose-dependent manner. The peak viral titer was determined to be $10^{6.9}$ PFU/ml in the vehicle-treated control. The

addition of 20 μM U0126 reduced the PEDV titer to $10^{3.8}$ PFU/ml (a 3-log reduction compared to that in the control). PD98059 slightly reduced the virus titer at the same concentration, and the comparable inhibitory effect on the virus titer was observed for PD98059 at 100 μM . The growth kinetics study further demonstrated that the overall process of PEDV replication was markedly delayed when cells were treated with either U0126 or PD98059 at their optimal respective concentrations (Fig. 5B). Consequently, these findings revealed that ERK1/2 activation is required for successful PEDV replication in cells.

To provide direct evidence for the involvement of the ERK cascades in the regulation of PEDV, Vero cells were transfected with small interfering RNA (siRNA) specific to ERK1/2 or a commercial control nonspecific siRNA as a negative control. At 24 h post-transfection, cells were infected with PEDV for 24 h and used to determine the amounts of ERK1/2 proteins and virus propagation (Fig. 6). The expression levels of ERK molecules were reduced by more than 60% after siRNA treatment compared to those untreated and treated with the control siRNA, indicating specific knockdown of

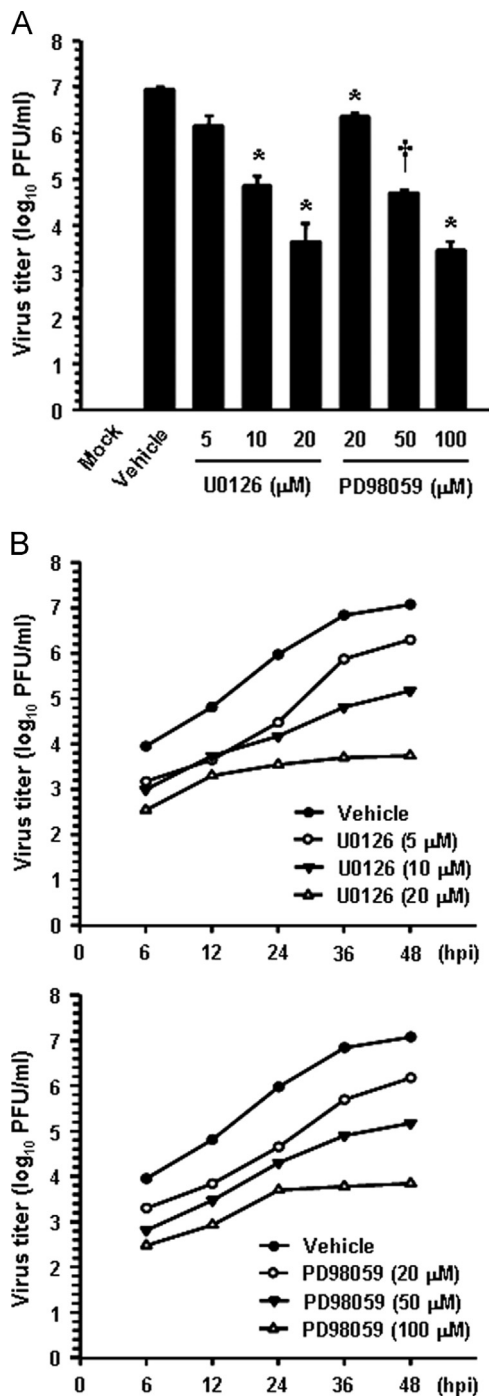


Fig. 5. Chemical inhibition reduces viral progeny production. (A) Vero cells were pretreated with DMSO, U0126, or PD98059 for 1 h and were mock or PEDV infected (MOI of 1). Vehicle or each inhibitor was present in the medium throughout the infection. At 48 hpi, the virus supernatants were collected and virus titers were determined. (B) Growth kinetics of PEDV upon treatment with each inhibitor was assessed exactly as for panel A. At the indicated time points postinfection, culture supernatants were harvested and virus titers were measured. Results are expressed as the mean values from triplicate wells and error bars represent standard deviations. *, $P=0.001$ to 0.05 ; †, $P < 0.001$.

ERK1/2 by siRNA (Fig. 6A). Furthermore, transfection of cells with ERK1/2-specific siRNA resulted in an almost 80% decrease in the number of PEDV-infected cells and an over 2-log reduction in virus titer compared to the mock- or nonspecific siRNA-transfected controls (B and C). The inhibitory effect of ERK1/2 siRNA on virus production was comparable to that of the chemical inhibition. Our data showed that knocked down expression of ERK1/2 diminishes

PEDV propagation, demonstrating an essential role of the ERK signaling pathway in PEDV replication.

Chemical inhibition of ERK1/2 activation suppresses PEDV replication at the early stage of infection but does not block virus internalization

To determine the point at which the two MEK inhibitors acted during PEDV infection, Vero cells were treated independently with each inhibitor at different time points post-infection. At 48 hpi, the levels of PEDV replication were measured indirectly as viral production by quantifying cells expressing the N protein through flow cytometry (Fig. 7A). Treatment of cells with 20 μ M U0126 for up to 4 hpi resulted in an 80% decrease in PEDV production when compared to the DMSO-treated control. Addition of U0126 between 6 and 12 hpi led to a 74–45% inhibition of PEDV infectivity. Consistently, the inhibitory profile of PD98059 was similar to that observed for U0126; however, it was less effective at the same concentration. In contrast, little or no significant reduction of PEDV propagation was identified when each inhibitor was added after 24 hpi. These results demonstrated that the effects of both inhibitors on PEDV production were exerted primarily at early steps in the virus life cycle, suggesting the importance of the ERK signaling pathway in the initial stage of infection.

Next, we sought to identify which step(s) of the replication cycle of PEDV was specifically targeted by inhibition of ERK activation. To address this issue, the earliest step, virus entry, was initially assessed with an internalization assay upon treatment with each MEK inhibitor. Vero cells were inoculated with PEDV at 4 °C for 1 h to allow virus attachment and were further maintained either at 4 °C or 37 °C to permit virus internalization in the presence of U0126 (20 μ M), PD98059 (100 μ M), or DMSO, followed by treatment of proteinase K to remove the remaining viruses on the cell surface. The serially diluted infected cells were subsequently subjected to an infectious center assay on uninfected Vero cell monolayers, and virus titers were measured 2 days later by plaque assay (Fig. 7B). Only minimal viral production was observed in cells maintained at 4 °C, which was likely due to an inefficient removal of the bound virus. The viral titers were nearly identical in cells treated with U0126, PD98059, or vehicle at 37 °C and were determined to be $10^{2.1}$, $10^{2.2}$ and $10^{2.4}$ PFU/ml, respectively, indicating no differences among treatment of these cells. These results indicated that neither U0126 nor PD98059 has any inhibitory effect on the virus entry process.

Chemical inhibition of ERK1/2 activation reduces viral protein translation and viral RNA transcription

Like other positive-sense RNA viruses, the PEDV genome is released into the cytoplasm following the uncoating process and immediately serves as a template for viral translation by the use of the translation machinery of the host cell. Early PEDV translation produces the replicase polyproteins that are proteolytically processed into nsps. Subsequently, the nonstructural replicase proteins mediate the *de novo* synthesis of viral RNA, including genomic RNA replication and sg mRNA transcription. The PEDV structural proteins are translated late in the cycle from their respective sg mRNA transcripts. Thus, to determine the functional mechanism of ERK1/2 regulation of PEDV infection on the post-entry steps, we first investigated whether viral protein translation was affected by ERK inhibition. For this approach, Vero cells were treated with each inhibitor for 1 h prior to infection, and then the inhibitors were independently present during the infection and subsequent incubation periods. The expression level of the PEDV N protein in the presence of each inhibitor or DMSO was evaluated at 48 hpi by Western blot analysis. Each chemical inhibition had a detrimental effect on viral protein production at different

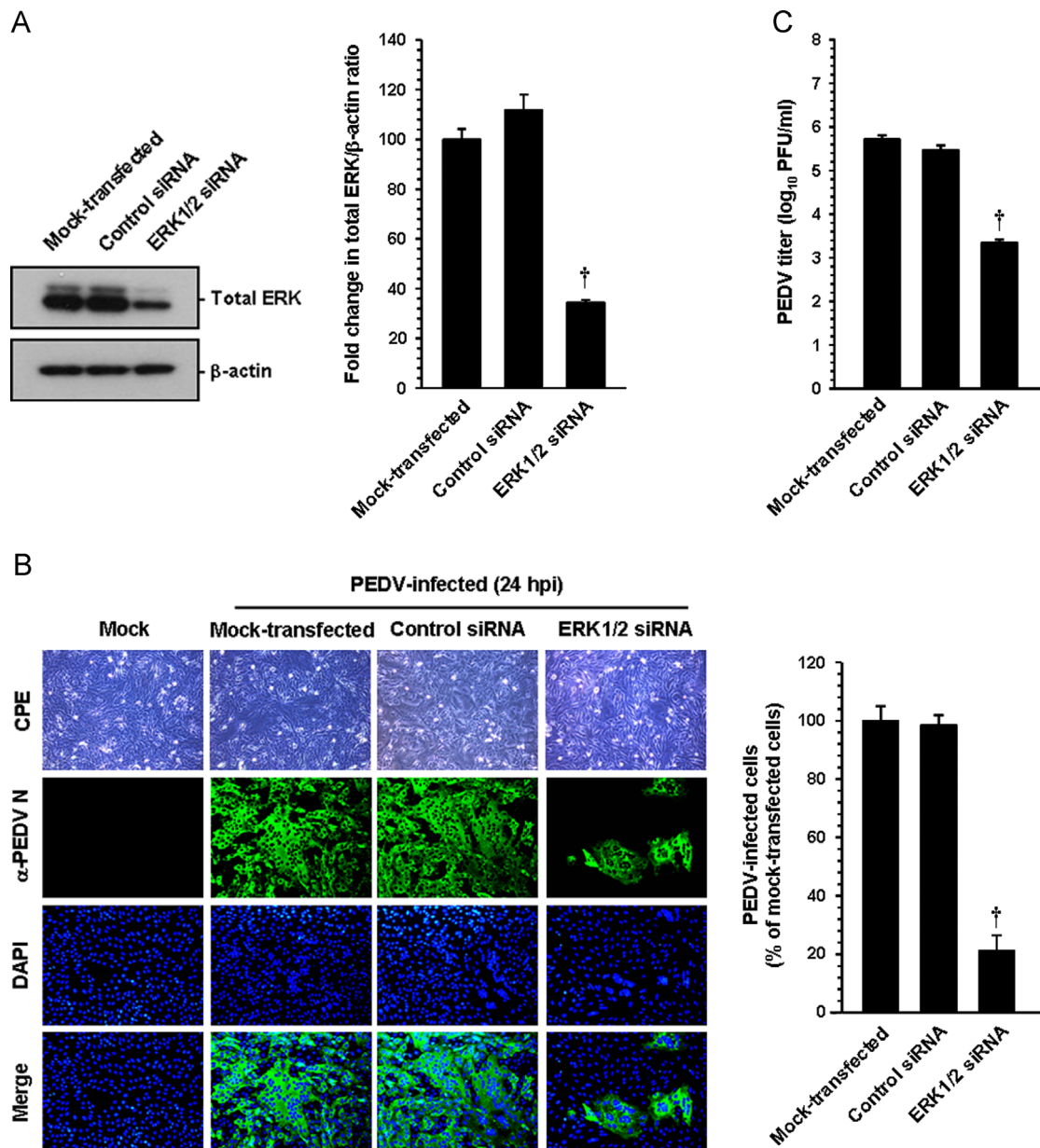


Fig. 6. ERK1/2 knockdown suppresses PEDV infection. Vero cells were transfected with 100 nM ERK-specific siRNA or control siRNA using Lipofectamine 2000 followed by PEDV infection at 24 h post transfection. (A) At 24 hpi, cellular lysates were prepared and subjected to immunoblotting using an antibody against the ERK protein. The blot was also reacted with anti-β-actin antibody to verify equal protein loading. ERK protein expression was quantitatively analyzed by densitometry and presented in terms of the relative density value to the β-actin gene, and fold changes in the total ERK:β-actin ratio are plotted. (B) PEDV-specific CPEs were observed daily and were photographed at 24 hpi using an inverted microscope at a magnification of 200× (first panels). For immunostaining, infected cells were fixed at 24 hpi and stained with anti-PEDV N antibody followed by Alexa green-conjugated goat anti-mouse secondary antibody (second panels). The cells were then counterstained with DAPI (third panels) and examined using a fluorescent microscope at 200× magnification. Viral production was assessed exactly as described in the legend of Fig. 4B. (C) The virus supernatants were collected at 24 hpi and viral titers were determined. Values shown are representative of the mean of three independent experiments and error bars represent standard deviations. †, $P < 0.001$.

concentrations (Fig. 8). Densitometric analysis of the Western blots revealed that the intracellular expression of the N protein was largely prevented by both inhibitors, and that a maximal ~80% inhibition was observed at the highest concentrations of U0126 and PD98059 used (Fig. 8). These data demonstrated the inhibitory effect on viral protein expression due to the specific action of each inhibitor on viral translation during PEDV replication.

Since synthesis of the viral nsps is required for viral RNA replication and transcription, it is conceivable that the suppression of viral protein expression could be a cascade-like result from the inhibition of viral RNA synthesis. Because PEDV infection produces two RNA entities, including genomic and subgenomic, we determined whether each ERK1/2 inhibitor specifically affected genome

replication and sg mRNA transcription. To answer this question, the relative levels of both genomic RNA and sg mRNA were assessed by quantitative real-time strand-specific RT-PCR in the presence or absence of U0126 or PD98059 upon PEDV infection. As shown in Fig. 9 A, both inhibitors greatly diminished viral RNA synthesis in a dose-dependent manner, showing a maximal 90% and 80% reduction in levels of viral genomic RNA and sg mRNA, respectively, compared to that in the DMSO-treated infected cells, respectively. The decrease in viral RNA levels after the addition of each inhibitor was not due to nonspecific inhibition of transcription, as the mRNA level of the internal GAPDH control remained unchanged in all samples (data not shown). The impairment of PEDV transcription in the presence of each inhibitor was further

confirmed by northern blot analysis (Fig. 9B). In untreated (lane 2) or vehicle-treated (lane 3) virus-infected cells, PEDV RNA synthesis was distinctly observed. Consistent with real-time RT-PCR data, a significant reduction in RNA-synthesizing activity occurred dose-dependently following treatment with U0126 (lanes 4 to 6) or PD98059 (lanes 7 to 9). Taken together, these results indicated that

both ERK inhibitors specifically suppress the synthesis of the PEDV genomic RNA and sg mRNA.

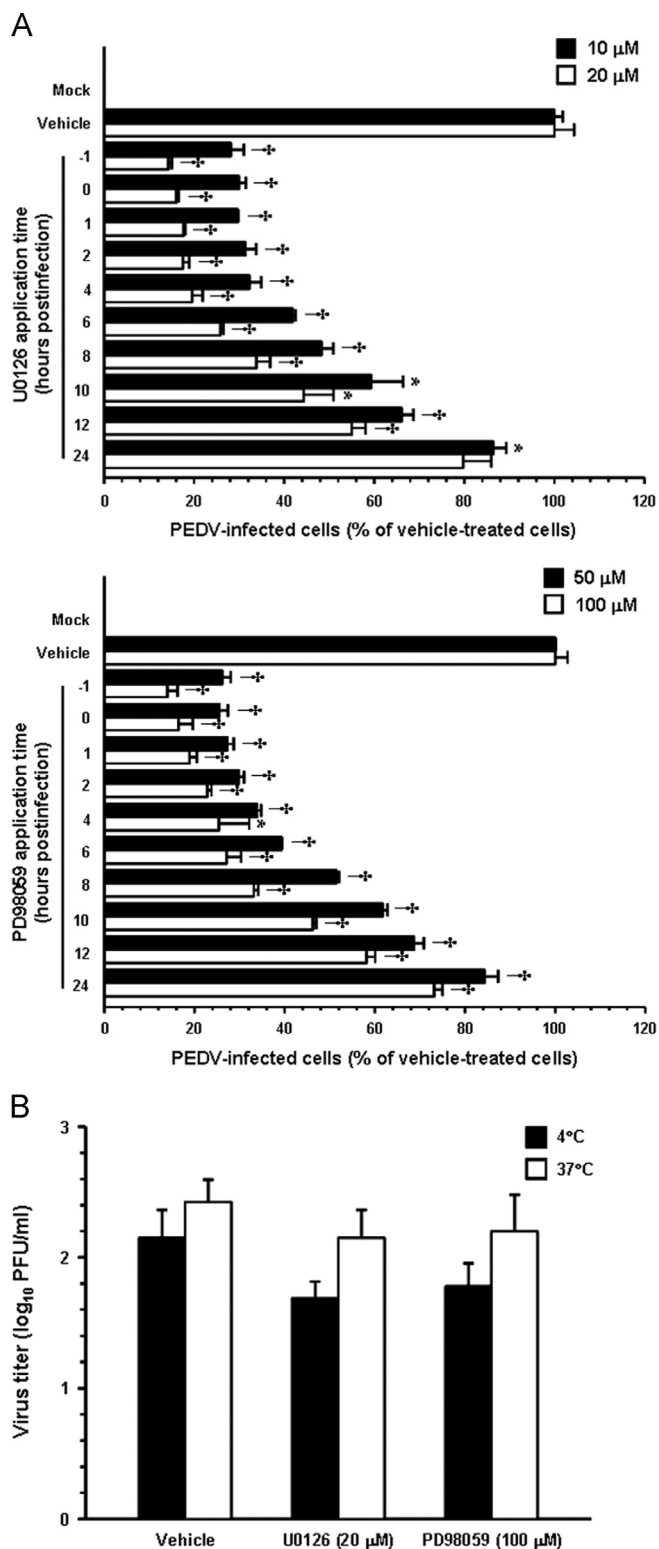
ERK1/2 activation is not involved in PEDV-induced apoptosis

The Raf/MEK/ERK signaling pathway manipulates various cell responses including different pro-proliferative and anti-proliferative events depending on stimuli. Growing evidence suggests that ERK activity is associated with classical markers of apoptosis execution, promoting apoptotic cell death in certain conditions (Cagnol and Chambard, 2010). Interestingly, PEDV has been shown to induce apoptosis *in vitro* and *in vivo* to facilitate viral replication and pathogenesis (Kim and Lee, 2014). Therefore, we speculated that the ERK pathway could play a role in the induction of apoptosis during PEDV replication. To examine whether ERK activation is required for PEDV-induced apoptosis, the process of PEDV-triggered apoptosis was assessed in the presence or absence of each ERK inhibitor using Annexin V/propidium iodide (PI) flow cytometry. Vero cells were treated with DMSO or each compound at the indicated concentrations followed by PEDV infection. At the indicated time points post-infection, the treated and infected cells were stained with Annexin V and PI and then examined using FACS flow cytometry to quantitatively determine the percentage of viable, apoptotic, and dead cells (Fig. 10A). Neither the vehicle nor the inhibitors tested caused significant apoptosis under our conditions. As expected, PEDV infection in the presence of DMSO induced a high level of apoptosis (Annexin V positive/PI negative) appearing at 6 hpi, and the percentage of early apoptotic cells increased with infection time. However, chemical inhibition of ERK1/2 activation was incapable of protecting cells from PEDV-induced apoptotic cell death. The percentage of early apoptotic cells in treatment of cells with either U0126 or PD98059 was comparable to that in vehicle-treated cells during the course of infection. Moreover, with chemical inhibition of ERK activation, nuclear translocation of AIF, a hallmark of PEDV-induced apoptosis, was still retained (Kim and Lee, 2014; Fig. 10B). These results indicated that the ERK signaling pathway is not involved in PEDV-mediated apoptosis and its mechanism.

Discussion

The significance of the interplay between host signaling pathways and numerous extracellular stimuli, including viral infection, has been extensively studied. Among these transduction signals, the ERK pathway plays multiple pivotal roles in almost all cell functions regulating cell fate (Cagnol and Chambard, 2010; Roux and Blenis, 2004; Shaul and Seger, 2007). Thus, the ability of ERK1/2 to control cell cycle progression is a reasonable target for the modulation of viral multiplication by acting at specific steps of the virus life cycle such as entry, gene transcription, protein expression, and progeny release (Cai et al., 2007; Lee and Lee, 2010; Moser and Schultz-Cherry, 2008; Planz et al.,

Fig. 7. ERK activation is required at an early stage of PEDV infection but does not affect virus internalization. (A) Vero cells were pretreated with DMSO, U0126 (10 and 20 μ M, upper panel), or PD98059 (50 and 100 μ M, lower panel) and were mock or PEDV (MOI of 1) infected. At the indicated times post-infection, each inhibitor was added to achieve a final concentration. At 48 hpi, virus-infected cells were fixed and virus infectivity was determined by quantifying the percentage of cells expressing N proteins through FACS. (B) Virus internalization assay. Vero cells were infected at an MOI of 1 at 4 °C for 1 h. After washing with cold PBS, infected cells were maintained in the presence or absence of each inhibitor either at 4 °C or 37 °C for an additional hour. Bound but non-internalized virus particles were removed by treatment with proteinase K. The infected cells were then serially diluted and plated onto Vero cells in 96-well tissue culture plates. At 2 days post-incubation, internalized viruses were titrated by plaque assay. Results are expressed as the mean values from triplicate wells and error bars represent standard deviations. *, $P=0.001$ to 0.05; †, $P<0.001$.



2001; Pleschka et al., 2001; Wei and Liu, 2009, Wong et al., 2005). Widespread ERK involvement appears to be a general characteristic for optimal viral infection, which beneficially functions as a global viral strategy to enhance its own replicative machinery. Despite decades of research, little about the intracellular signaling pathways involved in PEDV infection and pathogenesis has been deciphered. The present study demonstrated for the first time that ERK activation is required for efficient PEDV replication in cultured cells. In this study, we showed that PEDV strongly induces the activation of MAPK ERK1/2 *in vitro*, suggesting a crucial role of the ERK cascade during PEDV infection. Independent treatment with two ERK inhibitors and the knock down of ERK1/2 greatly impaired PEDV propagation. Moreover, chemical

inhibition of ERK activation resulted in significant attenuation of viral replication during post-entry steps, as determined by an overall down-regulation in viral protein expression, viral RNA synthesis, and progeny release. Altogether, it appears that the ERK signaling pathway regulates PEDV infection for competent viral reproduction in target cells.

As compared to infectious PEDV, the UV-inactivated virus also efficiently triggered ERK activation with the analogous phosphorylation kinetics, which suggested that the activation of ERK1/2 might be induced by the virus entry process, including virus-receptor interactions and the uncoating event. Furthermore, the productive growth of PEDV commenced at 12 hpi, as determined by the detection of a considerable amount of the viral protein; this corresponded to the proportionally down-regulated phosphorylation status of ERK1/2, and after 24 hpi, a reduction in the amount of pERK1/2 below the background level. In contrast, total ERK1/2 levels were found to remain consistent in cells throughout infection with non-irradiated or UV-irradiated PEDV. Altogether, it seems that the initial round of PEDV replication cycle, which likely occurs within 12 hpi, is essential for the maximal activation of the ERK signaling pathway. Interestingly, other nidoviruses have shown similar activation profiles of ERK1/2 that are independent of virus replication but are only in response to virus entry, suggesting a unique feature of the ERK pathway in the nidovirus biology (Cai et al., 2007; Lee and Lee, 2010). In addition, coxsackievirus and astrovirus were found to mediate rapid and ephemeral ERK activation observed within 10 to 15 min postinfection (Luo et al., 2002; Moser and Schultz-Cherry, 2008). However, in the current study, due to the relatively slow growth rate of PEDV, we were unable to determine how quickly the ERK pathway is activated following infection. The one-step growth curve indicated that the eclipse period appeared by 6 hpi and immediately after this, progeny viruses began to be detectable. For productive infection, PEDV particles must progressively proceed through a multiple-step cycle consisting of entry, uncoating, genome replication and transcription, viral translation, assembly, and progeny release. During the eclipse period, virus attachment and internalization occurs followed by uncoating to disassemble the viral capsid for genome release, which is now ready to initiate the replication cycle in the cytoplasm of infected cells. Although the exact mechanism to explain ERK1/2 activation following PEDV infection is unclear from the present study, it is tempting to speculate that virus-receptor interactions are responsible for ERK activation in PEDV-infected cells. The other possibility is that ERK

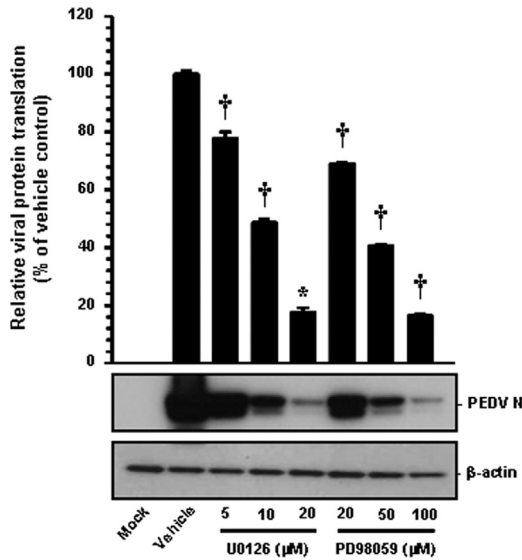


Fig. 8. Chemical inhibition of ERK1/2 activation impairs viral protein translation. Inhibitor-treated Vero cells were mock-infected or infected with PEDV (MOI of 1) for 1 h and were further cultivated in the presence or absence of each inhibitor. At 48 hpi, cellular lysates were collected, resolved by SDS-PAGE, transferred to a nitrocellulose membrane, and immunoblotted by using the antibody against the PEDV N protein. The blot was also reacted with mouse MAb against β-actin to verify equal protein loading. Each viral protein expression was quantitatively analyzed by densitometry in terms of the relative density value to the β-actin gene and inhibitor-treated sample results were compared to DMSO-control results. Values shown are representative of the mean from three independent experiments and error bars denote standard deviations. *, $P=0.001$ to 0.05 ; †, $P < 0.001$.

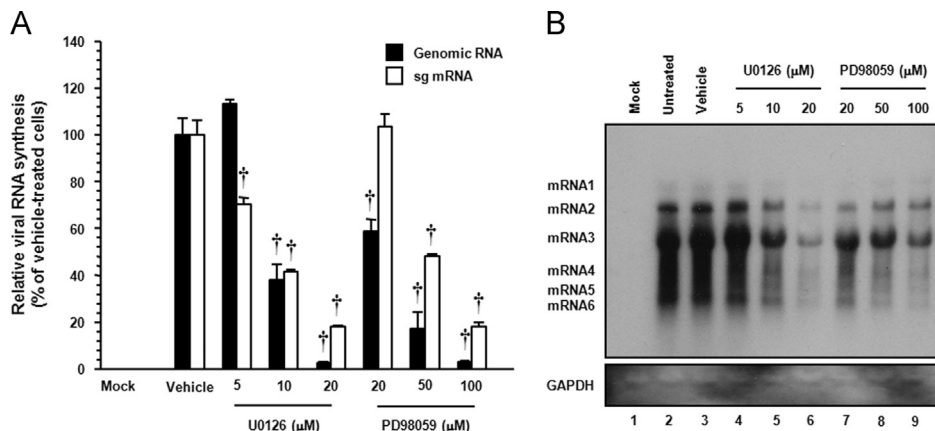


Fig. 9. Chemical inhibition of ERK1/2 activation interferes with viral RNA synthesis. Vero cells pretreated with DMSO, U0126, or PD98059 were mock-infected or infected with PEDV (MOI of 1) for 1 h and were incubated in the presence of DMSO or each inhibitor. (A) Total cellular RNA was extracted at 48 hpi, and strand-specific viral genomic RNA (black bars) and sg mRNA (white bars) were amplified by quantitative real-time RT-PCR. Viral positive-sense genomic RNA and sg mRNA were normalized to mRNA for monkey GAPDH, and relative quantities (RQ) of mRNA accumulation were evaluated. Inhibitor-treated sample results were compared with DMSO-treated results. Values shown are representative of the mean from three independent experiments and error bars denote standard deviations. †, $P < 0.001$. (B) The extracted RNA was also subjected to northern blot analysis using the specific oligonucleotide biotin-labeled probes against the PEDV-specific 3' UTR probe. Monkey GAPDH were used as a control to correct for variations in loading during viral RNA quantification. The positions of the genomic RNA and sg mRNAs are indicated next to the gel.

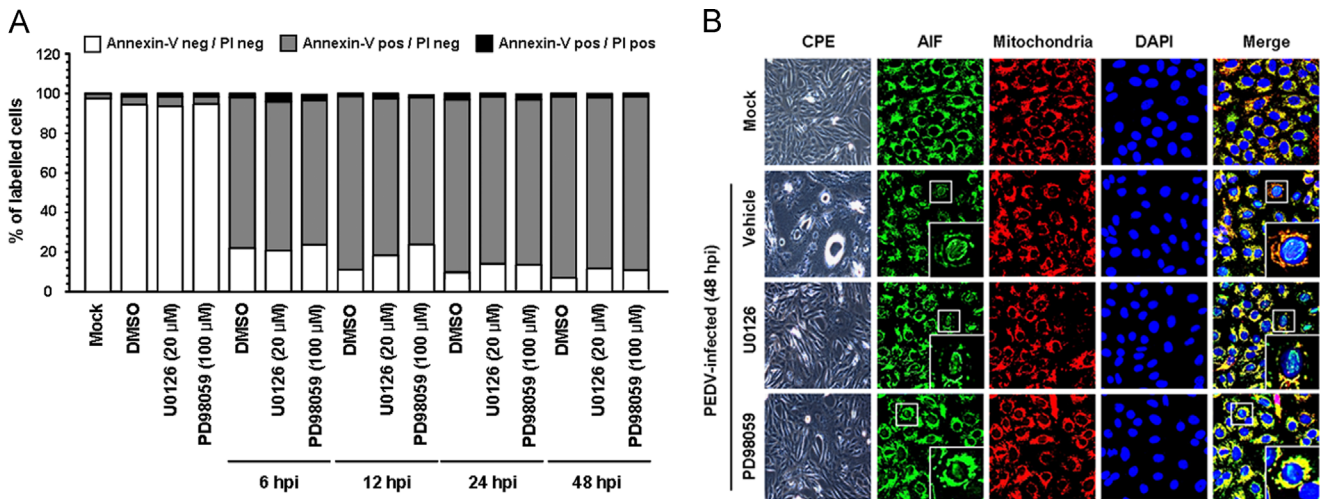


Fig. 10. Inhibition of ERK1/2 activation does not affect PEDV-induced apoptosis. Vero cells were treated with DMSO, U0126 (20 μM), or PD98059 (100 μM) for 1 h prior to infection and then mock-infected or infected with PEDV (MOI of 1) in the presence of DMSO or each inhibitor. (A) Cells were harvested at the indicated time points, dually labeled with Annexin V and PI, and subjected to FACS analysis. The graph represents the percentage of each quadrant, and the non-significant percentages of Annexin V-negative and PI-positive cells were excluded. (B) The treated and infected cells were also labeled with MitoTracker Red CMXRos (Red), fixed, and incubated with an anti-AIF antibody (green). AIF nuclear translocation is represented by the merged AIF and DAPI signals (turquoise), and residual mitochondrial colocalization is indicated by the merged AIF and mitochondrial marker (yellow). The inset images are enlarged versions of parts of the picture.

cascades are stimulated by virus particles entering through direct fusion with the cell membrane or by exposure to the disassembled viral proteins and the released genome after the uncoating process.

The data herein raises a question about the definite function of activated ERK1/2 during PEDV infection. A conceivable explanation for how ERK1/2 activation controls PEDV infection is that the ERK pathway regulates viral replication directly or indirectly. Independent treatment of PEDV-infected cells with each ERK inhibitor significantly suppressed individual postinternalization steps of the viral replication process, including viral RNA synthesis, protein expression, and virus production. Positive-sense RNA virus RdRps have been increasingly reported to be phosphoproteins activated by host proteins, suggesting regulation of viral RNA replication through phosphorylation of the polymerase protein (Jakubiec and Jupin, 2007). Moreover, previous studies have proposed that ERK1/2 activity might be necessary to phosphorylate or stabilize the viral RdRp, which are both required for the initiation of viral RNA replication (Luo et al., 2002; Moser and Schultz-Cherry, 2008). Therefore, a similar phosphorylation modification may activate the PEDV RdRp (nsp12) and could be indispensable for optimal viral RNA synthesis. ERK activation mediates apoptosis via either intrinsic or extrinsic pathways by the induction of mitochondrial cytochrome *c* release or caspase-8 activation, respectively (Cagnol and Chambard, 2010). Several viruses have been found to activate the ERK pathway to modulate apoptosis for contributing to their replication (Wong et al., 2005; Zampieri et al., 2007). We have previously demonstrated that PEDV promotes apoptotic cell death *in vitro* and *in vivo* to favor viral infection (Kim and Lee, 2014). However, the current study showed a negative correlation between the activation of ERK1/2 and apoptosis during PEDV infection. This result was anticipated because neither caspase activation nor cytochrome *c* release participated in the PEDV-triggered apoptosis pathway (Kim and Lee, 2014). Alternatively, ERK1/2 activation may be indirectly involved in PEDV infection by activating other cascades through crosstalk or by providing a signal to the downstream cellular transcription factors necessary for maximal virus propagation. Furthermore, in our experimental conditions, we were unable to completely eliminate viral replication during chemical inhibition. Therefore, if the indirect influence of ERK1/2 activity is the case,

ERK signaling could be one of the intracellular pathways important for PEDV replication.

In summary, our findings presented here revealed that PEDV infection activates ERK1/2 early in infection in cultured cells and that the activation of ERK molecules is required for efficient PEDV replication *in vitro*. However, viral processes or components underlying ERK activation remain to be determined. Although our data demonstrated the suppression of viral protein expression as well as viral RNA transcription by inhibiting ERK activation, the precise mechanism by which ERK activity modulates the PEDV replication cycle during infection is still unclear and, accordingly, this will be our next issue to address in future studies. A greater understanding of the precise role of ERK activation in the replication of PEDV will provide new insights into the molecular biology and pathogenesis of PEDV infection.

Material and methods

Cells, viruses, and reagents

Vero cells were cultured in alpha minimum essential medium (α-MEM; Invitrogen, Carlsbad, CA) with 5% fetal bovine serum (FBS; Invitrogen) and antibiotic-antimycotic solutions (100×; Invitrogen). The cells were maintained at 37 °C in a humidified 5% CO₂ incubator. PEDV strain SM98-1 was kindly provided by the Korean Animal and Plant Quarantine Agency and propagated in Vero cells as described previously (Hofmann and Wyler, 1988; Nam and Lee, 2010). Inactivation of PEDV was performed by UV irradiation of the virus suspension with 1000 mJ/cm² using a UV crosslinker (Stratagene, La Jolla, CA). Virus inactivation was confirmed by the inoculation of the UV-treated virus on Vero cells followed by N protein-specific staining as described below, and the inactivated virus was stored at −80 °C. The PEDV N protein-specific monoclonal antibody (MAb) was obtained from ChoogAng Vaccine Laboratory (CAVAC; Daejeon, South Korea). Antibodies specific for AIF and β-actin were purchased from Santa Cruz Biotechnology (Santa Cruz, CA). The MEK1/2 inhibitors U0126 and PD98059, antibodies against ERK1/2, phosphorylated ERK1/2

(pERK1/2), phosphorylated Elk-1 (pElk-1), and ERK-specific and unconjugated control siRNAs were obtained from Cell Signaling Technology (Danvers, MA).

Cell viability assay

The cytotoxic effects of reagents on Vero cells were analyzed using a colorimetric 3-(4,5-dimethylthiazol-2-yl)-2,5-diphenyltetrazolium bromide (MTT) assay (Sigma, St Louis, MO) to detect cell viability. Briefly, Vero cells were grown at 1×10^4 cells/well in a 96-well tissue culture plate with PD98059 or U0126 treatment for 24 h. After 1 day of incubation, 50 μ l of MTT solution (1.1 mg/ml) was added to each well, and the samples were incubated for an additional 4 h. The supernatant was then removed from each well, after which 150 μ l of DMSO was added to dissolve the colored formazan crystals produced by the MTT. The absorbance of the solution was measured at 540 nm using an enzyme-linked immunosorbent assay plate reader. All MTT assays were performed in triplicate.

Western blot analysis

Vero cells were grown in 6-well tissue culture plates for 1 day and were mock infected or infected with PEDV at a multiplicity of infection (MOI) of 1 or with an equal amount of UV-inactivated virus. At the indicated times, cells were harvested in 50 μ l of lysis buffer (0.5% TritonX-100, 60 mM β -glycerophosphate, 15 mM p -nitro phenyl phosphate, 25 mM MOPS, 15 mM, $MgCl_2$, 80 mM NaCl, 15 mM EGTA [pH 7.4], 1 mM sodium orthovanadate, 1 μ g/ml E64, 2 μ g/ml aprotinin, 1 μ g/ml leupeptin, and 1 mM PMSF) and sonicated on ice 5 times for 1 s each. Homogenates were lysed for 30 min on ice, and clarified by centrifugation at $15,800 \times g$ (Eppendorf centrifuge 5415R, Hamburg, Germany) for 30 min at 4 °C. To examine the effect of ERK inhibition on PEDV replication, cells were pretreated independently with each MEK inhibitor for 1 h and then infected with PEDV at an MOI of 1. The virus-inoculated cells were further propagated in the presence of U0126 (5–20 μ M), PD98059 (20–100 μ M), or DMSO (0.5%; vehicle control) and cell lysates were prepared with lysis buffer at 48 h hpi. The total protein concentrations in the supernatants were determined using a BCA protein assay (Pierce, Rockford, IL). Equal amounts of total protein were separated on a NuPAGE 4–12% gradient Bis-Tris gel (Invitrogen) under reducing conditions and electrotransferred onto an Immobilon-P (Millipore, Bedford, MA). The membranes were subsequently blocked with 3% powdered skim milk (BD Biosciences, Bedford, MA) in TBS (10 mM Tris-HCl [pH 8.0], 150 mM NaCl) with 0.05% Tween-20 (TBST) at 4 °C for 2 h and incubated at 4 °C overnight with the primary antibody against pERK1/2, ERK1/2, pElk-1, PEDV N, or β -actin. The blots were then incubated with the corresponding secondary HRP-labeled antibodies at a dilution of 1:5000 for 2 h at 4 °C. Proteins were visualized using enhanced chemiluminescence (ECL) reagents (GE Healthcare, Piscataway, NJ) according to the manufacturer's instructions. Ratios of phosphorylated/total ERK1/2 and phosphorylated Elk-1/ β -actin were compared by densitometry of the corresponding bands using a computer densitometer with the Wright Cell Imaging Facility (WCIF) version of the ImageJ software package (<http://www.uhnresearch.ca/facilities/wcif/imagej/>). To quantify viral protein production, the band densities of PEDV N proteins were quantitatively analyzed using a computer densitometer with ImageJ software in terms of the density value relative to that of the β -actin gene.

Fast activated cell-based ELISA (FACE)

FACE kit was obtained from Active Motif (Carlsbad, CA) and was used to determine the levels of ERK1/2 MAPK activation according to the manufacturer's protocols. Briefly, Vero cells seeded in 96-well tissue culture plate were grown for 1 day and were infected

with PEDV or UV-inactivated virus as described above. At the indicated times, infected cells were fixed with 4% formaldehyde. In addition, Vero cells were pretreated independently with each MEK inhibitor for 1 h followed by PEDV infection and fixed at 12 hpi. After washing and blocking, cells were reacted overnight with an anti-ERK1/2 or anti-phospho-ERK1/2 antibody. Following incubation with an HRP-conjugated secondary antibody, a colorimetric analysis was performed, with the absorbance of the solution determined at 450 nm using a spectrophotometer.

Immunofluorescence assay (IFA)

Vero cells grown on microscope coverslips placed in 6-well tissue culture plates were mock infected or infected with PEDV or UV-inactivated PEDV at an MOI of 1 for the indicated times. To assess the effect of MEK inhibitors on PEDV infection, cells were pretreated with U0126, PD98059, or DMSO for 1 h and then infected with PEDV. Virus-infected cells were subsequently maintained in the presence of vehicle or each inhibitor for 48 h. All treated cells were fixed with 4% paraformaldehyde for 10 min at RT and permeabilized with 0.2% Triton X-100 in PBS at RT for 10 min. The cells were blocked with 1% bovine serum albumin (BSA) in PBS for 30 min at RT and then incubated with pERK1/2 or PEDV N-specific MAb for 2 h. After being washed five times in PBS, the cells were incubated for 1 h at RT with a goat anti-mouse secondary antibody conjugated to Alexa Fluor 488 (Invitrogen), followed by counterstaining with 4',6-diamidino-2-phenylindole (DAPI; Sigma). The coverslips were mounted on microscope glass slides in mounting buffer and cell staining was visualized using a fluorescent Leica DM IL LED microscope (Leica, Wetzlar, Germany). To examine AIF subcellular localization under the chemical inhibition of PEDV-induced ERK activation, MitoTracker Red CMXRos (200 nM; Invitrogen) was added to vehicle or MEK inhibitor-treated and virus-infected Vero cells and left for 45 min at 37 °C prior to fixation. The cells were then stained with AIF-specific antibody as described above, and cell staining was analyzed using a Confocal Laser Scanning microscope (Carl Zeiss, Göttingen, Germany).

Fluorescence-activated cell sorting (FACS) analysis

Quantification of PEDV-infected cells upon independent treatment of each MEK inhibitor was analyzed by flow cytometry. Vero cells were pretreated with U0126, PD98059, or DMSO for 1 h, infected with PEDV, and subsequently maintained in the presence of vehicle or each inhibitor. Virus-infected cells were trypsinized at 48 hpi and centrifuged at $250 \times g$ (Hanil Centrifuge FLETA 5) for 5 min. The cell pellet was washed with cold washing buffer (1% BSA and 0.1% sodium azide in PBS), and 10^6 cells were resuspended in 1% formaldehyde solution in cold wash buffer for fixation at 4 °C in the dark for 30 min followed by centrifugation and incubation of the pellet in 0.2% Triton X-100 in PBS at 37 °C for 15 min for permeabilization. After centrifugation, the cell pellet was resuspended in a solution of the primary anti-N MAb and the mixture was incubated at 4 °C for 30 min. The cells were washed and allowed to react with an Alexa Fluor 488-conjugated anti-mouse IgG secondary antibody at 4 °C for 30 min in the dark. The stained cells were washed again and analyzed on a FACSAria III flow cytometer (BD Biosciences).

Time course of MEK1/2 inhibitor treatment

Vero cells were infected with PEDV, at an MOI of 1. At –1, 0, 1, 2, 4, 6, 8, 10, 12, or 24 hpi, inhibitors were added to give the indicated final concentration over the remainder of the time course experiment. The PEDV-infected and inhibitor-treated cells were further

maintained and the infection was terminated at 48 hpi by fixing the monolayers with 4% paraformaldehyde for 10 min at RT. The fixed cells were subjected to FACS analysis to assess the presence of PEDV infection as described above.

Virus titration

Vero cells were PEDV infected and treated with U0126, PD98059, or DMSO. The culture supernatants were collected at different time points (6, 12, 24, 36, and 48 hpi) and stored at -80°C . The PEDV titer was determined by plaque assay using Vero cells as described previously (Nam and Lee, 2010) and quantified as plaque-forming units (PFU) per ml.

Virus internalization assay

An internalization assay was performed as described previously with some modifications (Cai et al., 2007). Briefly, Vero cells grown in 6-well culture plate were pretreated and infected with PEDV at an MOI of 1 at 4°C for 1 h in the presence of respective compounds. Unbound viruses were then washed with PBS, and the cells were either incubated at 4°C or 37°C in the presence of each MEK1/2 inhibitor or DMSO for 1 h, followed by treatment with proteinase K (0.5 mg/ml) at 4°C for 45 min to remove the bound but uninternalized virus particles. The PEDV-infected cells were then serially diluted in culture medium and added onto fresh Vero cell monolayers in 96-well tissue culture plates. At 48 h post-incubation, internalized viruses were titrated using plaque assay and quantified as PFU per ml.

Quantitative real-time RT-PCR

Vero cells were incubated with each MEK1/2 inhibitor or DMSO for 1 h prior to infection and then inoculated with PEDV at an MOI of 1 for 1 h at 37°C . The virus inoculum was subsequently removed and the infected cells were maintained in fresh medium containing U0126, PD98059, or DMSO for 48 h. Total RNA was extracted from lysates of the infected cells at 48 hpi using TRIzol reagent (Invitrogen) and treated with DNase I (TaKaRa, Otsu, Japan) according to the manufacturer's instructions. The concentrations of the extracted RNA were measured using a NanoVue spectrophotometer (GE Healthcare). Quantitative real-time RT-PCR was conducted using a Thermal Cycler Dice Real Time System (TaKaRa) with gene-specific primer sets described previously (Kim and Lee, 2013). The RNA levels of viral genes were normalized to that of mRNA for the glyceraldehyde-3-phosphate dehydrogenase (GAPDH) gene, and relative quantities (RQ) of mRNA accumulation were evaluated using the $2^{-\Delta\Delta\text{Ct}}$ method. To detect alterations in the genomic RNA and sg mRNA levels in the presence of each MEK1/2 inhibitor during PEDV infection, the results obtained using inhibitor-treated samples were compared to those of DMSO-treated results.

Northern blotting

Vero cells were pretreated with each inhibitor for 1 h followed by PEDV inoculation and were maintained as described above. Total RNA was extracted from lysates of the infected cells at 48 hpi using TRIzol reagent and treated with DNase I. Northern blotting was conducted by the NorthernMax Kit (Ambion, Austin, TX) according to the manufacturer's instructions. Samples of total RNA (5 μg) were loaded and separated by electrophoresis through Denaturing Gel Buffer-containing 1% agarose gel. The separated total RNA was then transferred to a BrightStar-Plus nylon membrane (Ambion) for 3 h and cross-linked by UV light for 5 min. Pre-hybridization was performed at 42°C for 40 min followed by

detection using the PEDV-specific 3' UTR probe (5'-GCCGATCTT-TAATTACTCGTGCAAAGGTTTAGATGAAAAGGTACTGCGTCCCC-3') or monkey glyceraldehyde-3-phosphate dehydrogenase (GAPDH) (5'-GCCTGGCTGTTAGGTATCGGTGAGG-3'). The blot was hybridized to biotin-labeled oligonucleotide probes in ULTRAhyb reagent at 42°C overnight and washed twice with low-stringency blocking buffer and wash buffer. Target viral RNAs were detected by the BrightStar BioDetect Kit (Ambion) according to the manufacturer's protocols. The membrane was incubated with alkaline phosphatase-conjugated streptavidin followed by reaction with the chemiluminescent substrate CDP-STAR (Ambion). The overlaid films were obtained by exposure in a dark cassette box in a dark room.

Knocked down expression of ERK by siRNA

Vero cells were transfected with 100 nM siRNA targeting ERK1/2 or control siRNA using Lipofectamin 2000 (Invitrogen) according to the manufacturer's protocols. At 24 h post transfection, cells were infected with PEDV at an MOI of 1 for 24 h. ERK1/2 proteins were detected by Western blot analysis and quantitatively analyzed using a computer densitometer as described above. At 24 hpi, the infected cells were fixed and subjected to PEDV N-specific IFA, while the culture supernatants were harvested and subjected to virus titration by plaque assay.

Annexin V and PI staining assay

Vero cells were pretreated with each inhibitor for 1 h and then mock infected or infected with PEDV at an MOI of 1. The virus-inoculated cells were further propagated in the presence of U0126 (20 μM), PD98059 (100 μM), or DMSO. Phosphatidylserine exposure was determined by measuring Annexin V binding at the indicated times using an Alexa Fluor 488 Annexin V/Dead Cell Apoptosis Kit (Invitrogen), according to the manufacturer's protocol. In brief, cells were harvested, washed with cold PBS, and suspended in 100 μl $1 \times$ annexin-binding buffer. The cells were then incubated with Alexa Fluor 488-conjugated Annexin V and PI at RT for 15 min in the dark. Following the incubation period, 400 μl of annexin-binding buffer was added to each sample, and the samples were mixed gently and kept on ice. The fluorescent signals of Annexin V and PI were detected at channels FL-1 and FL-2, respectively, and analyzed using a FACS Aria III flow cytometer. Cells negative for PI uptake and positive for Annexin V were considered apoptotic.

Statistical analysis

All statistical analyses were performed using Student's *t*-test, and *P*-values of less than 0.05 were considered statistically significant.

Acknowledgment

This research was supported by Basic Science Research Program through the National Research Foundation of Korea (NRF) funded by the Ministry of Education, Science and Technology (NRF-2012R1A1A2039746).

References

- Alessi, D.R., Cuenda, A., Cohen, P., Dudley, D.T., Saltiel, A.R., 1995. PD 098059 is a specific inhibitor of the activation of mitogen-activated protein kinase kinase *in vitro* and *in vivo*. *J. Biol. Chem.* 270, 27489–27494.
- Cagnol, S., Chambard, J.C., 2010. ERK and cell death: mechanisms of ERK-induced cell death-apoptosis, autophagy and senescence. *FEBS J.* 277, 2–21.

- Cai, Y., Liu, Y., Zhang, X., 2007. Suppression of coronavirus replication by inhibition of the MEK signaling pathway. *J. Virol.* 81, 446–456.
- Chasey, D., Cartwright, S.F., 1978. Virus-like particles associated with porcine epidemic diarrhoea. *Res. Vet. Sci.* 25, 255–256.
- Chen, J.F., Sun, D.B., Wang, C.B., Shi, H.Y., Cui, X.C., Liu, S.W., Qiu, H.J., Feng, L., 2008. Molecular characterization and phylogenetic analysis of membrane protein genes of porcine epidemic diarrhoea virus isolates in China. *Virus Genes* 36, 355–364.
- Davis, S., Vanhoutte, P., Pages, C., Caboche, J., Laroche, S., 2000. The MAPK/ERK cascade targets both Elk-1 and cAMP response element-binding protein to control long-term potentiation-dependent gene expression in the dentate gyrus *in vivo*. *J. Neurosci.* 20, 4563–4572.
- Deboucq, P., Pensaert, M., 1980. Experimental infection of pigs with a new porcine enteric coronavirus, CV 777. *Am. J. Vet. Res.* 41, 219–223.
- Duarte, M., Tobler, K., Bridgen, A., Rasschaert, D., Ackermann, M., Laude, H., 1994. Sequence analysis of the porcine epidemic diarrhoea virus genome between the nucleocapsid and spike protein genes reveals a polymorphic ORF. *Virology* 198, 466–476.
- Favata, M.F., Horiuchi, K.Y., Manos, E.J., Daulerio, A.J., Stradley, D.A., Feeser, W.S., Van Dyk, D.E., Pitts, W.J., Earl, R.A., Hobbs, F., Copeland, R.A., Magolda, R.L., Scherle, P. A., Trzaskos, J.M., 1998. Identification of a novel inhibitor of mitogen-activated protein kinase. *J. Biol. Chem.* 273, 18623–18632.
- Garrington, T.P., Johnson, G.L., 1999. Organization and regulation of mitogen-activated protein kinase signaling pathways. *Curr. Opin. Cell Biol.* 11, 211–218.
- Hofmann, M., Wyler, R., 1988. Propagation of the virus of porcine epidemic diarrhoea in cell culture. *J. Clin. Microbiol.* 26, 2235–2239.
- Jakubiec, A., Jupin, I., 2007. Regulation of positive-strand RNA virus replication: the emerging role of phosphorylation. *Virus Res.* 129, 73–79.
- Kim, Y., Lee, C., 2014. Porcine epidemic diarrhoea virus induces caspase-independent apoptosis through activation of mitochondrial apoptosis-inducing factor. *Virology* 460–461, 180–193.
- Kim, Y., Lee, C., 2013. Ribavirin efficiently suppresses porcine nidovirus replication. *Virus Res.* 171, 44–53.
- Kocherhans, R., Bridgen, A., Ackermann, M., Tobler, K., 2001. Completion of the porcine epidemic diarrhoea coronavirus (PEDV) genome sequence. *Virus Genes* 23, 137–144.
- Kweon, C.H., Kwon, B.J., Jung, T.S., Kee, Y.J., Hur, D.H., Hwang, E.K., et al., 1993. Isolation of porcine epidemic diarrhoea virus (PEDV) in Korea. *Korean J. Vet. Res.* 33, 249–254.
- Lai, M.C., Perlman, S., Anderson, L.J., 2007. Coronaviridae. In: Knipe, D.M., Howley, P.M., Griffin, D.E., Martin, M.A., Lamb, R.A., Roizman, B., Straus, S.E. (Eds.), *Fields Virology*, 5th ed. Lippincott Williams & Wilkins, Philadelphia, PA, pp. 1305–1336.
- Lee, S., Lee, C., 2014. Outbreak-related porcine epidemic diarrhoea virus strains similar to US strains, South Korea, 2013. *Emerg. Infect. Dis.* 20, 1223–1226.
- Lee, S., Ko, D.H., Kwak, S.K., Lim, C.H., Moon, S.U., Lee, D.S., Lee, C., 2014a. Reemergence of porcine epidemic diarrhoea virus on Jeju Island. *Korean J. Vet. Res.* 54, 185–188.
- Lee, S., Park, G.S., Shin, J.H., Lee, C., 2014b. Full-genome sequence analysis of a variant strain of porcine epidemic diarrhoea virus in South Korea. *Genome Announc.* 2, e01116–14.
- Lee, Y.J., Lee, C., 2010. Porcine reproductive and respiratory syndrome virus replication is suppressed by inhibition of the extracellular signal-regulated kinase (ERK) signaling pathway. *Virus Res.* 152, 50–58.
- Li, W., Li, H., Liu, Y., Pan, Y., Deng, F., Song, Y., Tang, X., He, Q., 2012. New variants of porcine epidemic diarrhoea virus, China, 2011. *Emerg. Infect. Dis.* 18, 1350–1353.
- Lim, B.K., Nam, J.H., Gil, C.O., Yun, S.H., Choi, J.H., Kim, D.K., Jeon, E.S., 2005. Coxsackievirus B3 replication is related to activation of the late extracellular signal-regulated kinase (ERK) signal. *Virus Res.* 113, 153–157.
- Lin, C.N., Chung, W.B., Chang, S.W., Wen, C.C., Liu, H., Chien, C.H., Chiou, M.T., 2014. US-like strain of porcine epidemic diarrhoea virus outbreaks in Taiwan, 2013–2014. *J. Vet. Med. Sci.* 76, 1297–1299.
- Luo, H., Yanagawa, B., Zhang, J., Luo, Z., Zhang, M., Esfandiari, M., Carthy, C., Wilson, J.E., Yang, D., McManus, B.M., 2002. Coxsackievirus B3 replication is reduced by inhibition of the extracellular signal-regulated kinase (ERK) signaling pathway. *J. Virol.* 76, 365–373.
- Madson, D.M., Magstadt, D.R., Arruda, P.H., Hoang, H., Sun, D., Bower, L.P., Bhandari, M., Burrough, E.R., Gauger, P.C., Pillatzki, A.E., Stevenson, G.W., Wilberts, B.L., Brodie, J., Harmon, K.M., Wang, C., Main, R.G., Zhang, J., Yoon, K.J., 2014. Pathogenesis of porcine epidemic diarrhoea virus isolate (US/Iowa/18984/2013) in 3-week-old weaned pigs. *Vet. Microbiol.* 174, 60–68.
- Marjuki, H., Alam, M.I., Ehrhardt, C., Wagner, R., Planz, O., Klenk, H.D., Ludwig, S., Pleschka, S., 2006. Membrane accumulation of influenza A virus hemagglutinin triggers nuclear export of the viral genome via protein kinase C α -mediated activation of ERK signaling. *J. Biol. Chem.* 281, 16707–16715.
- Mole, B., 2013. Deadly pig virus slips through US borders. *Nature* 499, 388.
- Moser, L.A., Schultz-Cherry, S., 2008. Suppression of astrovirus replication by an ERK1/2 inhibitor. *J. Virol.* 82, 7475–7482.
- Nam, E., Lee, C., 2010. Contribution of the porcine aminopeptidase N (CD13) receptor density to porcine epidemic diarrhoea virus infection. *Vet. Microbiol.* 144, 41–50.
- Oldham, J., 1972. Letter to the editor. *Pig Farming* 10, 72–73.
- Pensaert, M.B., de Bouck, P., 1978. A new coronavirus-like particle associated with diarrhoea in swine. *Arch. Virol.* 58, 243–247.
- Pensaert, M.B., de Bouck, P., Reynolds, D.J., 1981. An immunoelectron microscopic and immunofluorescent study on the antigenic relationship between the coronavirus-like agent, CV 777, and several coronaviruses. *Arch. Virol.* 68, 45–52.
- Pijpers, A., van Nieuwstadt, A.P., Terpstra, C., Verheijden, J.H., 1993. Porcine epidemic diarrhoea virus as a cause of persistent diarrhoea in a herd of breeding and finishing pigs. *Vet. Rec.* 132, 129–131.
- Planz, O., Pleschka, S., Ludwig, S., 2001. MEK-specific inhibitor U0126 blocks spread of Borna disease virus in cultured cells. *J. Virol.* 75, 4871–4877.
- Pleschka, S., Wolff, T., Ehrhardt, C., Hobom, G., Planz, O., Rapp, U.R., Ludwig, S., 2001. Influenza virus propagation is impaired by inhibition of the Raf/MEK/ERK signalling cascade. *Nat. Cell Biol.* 3, 301–305.
- Puranaveja, S., Poolperm, P., Lertwatcharasarakul, P., Kesdaengsakonwut, S., Boonsoongnern, A., Urairong, K., Kitikoon, P., Choojai, P., Kedkovid, R., Teankum, K., Thanawongnuwech, R., 2009. Chinese-like strain of porcine epidemic diarrhoea virus, Thailand. *Emerg. Infect. Dis.* 15, 1112–1115.
- Roux, P.P., Blenis, J., 2004. ERK and p38 MAPK-activated protein kinases: a family of protein kinases with diverse biological functions. *Microbiol. Mol. Biol. Rev.* 68, 320–344.
- Saif, L.J., Pensaert, M.B., Sestack, K., Yeo, S.G., Jung, K., 2012. Coronaviruses. In: Straw, B.E., Zimmerman, J.J., Karriker, L.A., Ramirez, A., Schwartz, K.J., Stevenson, G.W. (Eds.), *Diseases of Swine*, 10th ed. Wiley-Blackwell, Ames, IA, pp. 501–524.
- Schümann, M., Döbelstein, M., 2006. Adenovirus-induced extracellular signal-regulated kinase phosphorylation during the late phase of infection enhances viral protein levels and virus progeny. *Cancer Res.* 66, 1282–1288.
- Shaul, Y.D., Seger, R., 2007. The MEK/ERK cascade: from signaling specificity to diverse functions. *Biochim. Biophys. Acta.* 1773, 1213–1226.
- Shibata, I., Tsuda, T., Mori, M., Ono, M., Sueyoshi, M., Urano, K., 2000. Isolation of porcine epidemic diarrhoea virus in porcine cell cultures and experimental infection of pigs of different ages. *Vet. Microbiol.* 72, 173–182.
- Stevenson, G.W., Hoang, H., Schwartz, K.J., Burrough, E.R., Sun, D., Madson, D., Cooper, V.L., Pillatzki, A., Gauger, P., Schmitt, B.J., Koster, L.G., Killian, M.L., Yoon, K.J., 2013. Emergence of Porcine epidemic diarrhoea virus in the United States: clinical signs, lesions, and viral genomic sequences. *J. Vet. Diagn. Invest.* 25, 649–654.
- Sun, R.Q., Cai, R.J., Chen, Y.Q., Liang, P.S., Chen, D.K., Song, C.X., 2012. Outbreak of porcine epidemic diarrhoea in suckling piglets, China. *Emerg. Infect. Dis.* 18, 161–163.
- Takahashi, K., Okada, K., Ohshima, K., 1983. An outbreak of swine diarrhoea of a new-type associated with coronavirus-like particles in Japan. *Jpn. J. Vet. Sci.* 45, 829–832.
- Wang, J., Shen, Y.H., Utama, B., Wang, J., LeMaire, S.A., Coselli, J.S., Vercellotti, G.M., Wang, X.L., 2006. HCMV infection attenuates hydrogen peroxide induced endothelial apoptosis-involvement of ERK pathway. *FEBS Lett.* 580, 2779–2787.
- Wei, L., Liu, J., 2009. Porcine circovirus type 2 replication is impaired by inhibition of the extracellular signal-regulated kinase (ERK) signaling pathway. *Virology* 386, 203–209.
- Wong, W.R., Chen, Y.Y., Yang, S.M., Chen, Y.L., Horng, J.T., 2005. Phosphorylation of PI3K/Akt and MAPK/ERK in an early entry step of enterovirus 71. *Life Sci.* 78, 825–90.
- Zampieri, C.A., Fortin, J.F., Nolan, G.P., Nabel, G.J., 2007. The ERK mitogen-activated protein kinase pathway contributes to Ebola virus glycoprotein-induced cytotoxicity. *J. Virol.* 81, 1230–1240.